

Fractal Rosette: A Stable Space-Ground Network Structure in Mega-constellation

Yuanjie Li, Hewu Li, Lixin Liu, Wei Liu, Jiayi Liu, Jianping Wu,

Qian Wu, Jun Liu, Zeqi Lai, Guojie Fan

Institute for Network Sciences and Cyberspace, Tsinghua University

ABSTRACT

We present F-Rosette, a stable space-ground network structure for low-earth orbit (LEO) satellite mega-constellations at scale. Due to the dynamic many-to-many space-ground mapping in high mobility, existing LEO mega-constellations with IP protocol stack suffer from frequent user IP address changes (every 133–510s per user) and network routing re-convergence (thus $\leq 20\%$ network usability). To provably stabilize the space-ground network under high dynamics, F-Rosette aligns the network design in the cyberspace with the mega-constellations in the physical world. It devises a recursively stable network structure over the Rosette constellation, decouples the hierarchical network addresses from mobility for stability, and aligns the geographical routing on the ground with the topological routing in space for efficiency and high usability. Our hardware-in-the-loop, trace-driven emulations validate F-Rosette’s stability, near-optimal routing ($\leq 1.4\%$ additional delays), and affordable overhead ($< 1\%$ CPU, $< 2\text{MB}$ memory) for resource-constrained satellites.

1 INTRODUCTION

The future Internet is up in the sky. Since 2019, we have witnessed a rocket-fast deployment of the low-earth-orbit (LEO) satellite mega-constellations, including SpaceX Starlink [1], Amazon Kuiper [2], Telesat [3], OneWeb [4], to name a few. Compared to the traditional satellite networks, these LEO mega-constellations promise ultra-low network latency and high throughput that are competitive to the terrestrial networks. Moreover, with massive satellites, these mega-constellations offer the global Internet coverage to users that were not easily reachable by terrestrial networks, such as those in rural areas and the ocean.

This work asks a simple question: *How to enable a usable network in mega-constellations to serve the terrestrial users?* Despite the rapid deployments of LEO mega-constellations, inter-connecting satellites for network services is still at early designs on a tiny scale (such as Starlink’s “Better Than Nothing” plan [5] and initial inter-satellite link test [6, 7]). With massive mobile LEO satellites and their relative motions to numerous terrestrial users on a rotating earth, it is open to question whether the traditional wisdom of satellite network designs are still suitable for the mega-constellations.

A grand challenge for a usable space-ground network is to guarantee its *stability* under satellites and earth’s high mobility. Unlike the traditional satellite and terrestrial networks, the LEO network exhibits *highly dynamic many-to-many mapping* between the moving satellites and terrestrial users. Each LEO satellite can cover $\approx 100,000$ users, while each terrestrial user has visibility to ≈ 20 satellites in mega-constellations [8]. The high satellite mobility and earth’s rotation force the terrestrial users to frequently re-associate to new satellites. Therefore, the network topology between the space and ground repetitively changes, which results in frequent network address changes and routing protocol re-convergence. Our projection of mega-constellations running IP protocols shows that (§2.2), every terrestrial user switches its IP address every 133–510s (with 2,082–7,961 users changing IP addresses every second), and the network usability decreases to $\leq 20\%$ with frequent routing re-convergence. Even worse, both stability issues are amplified as mega-constellations scale to massive satellites.

The fundamental cause of the above unstable space-ground network is the mismatch between the network in the virtual cyberspace and mega-constellations in the physical world. On one hand, classical mega-constellations primarily focus on offering good coverage, but neglects the demands of stable network topology, addressing, and routing. On the other hand, most satellite networks in the virtual cyberspace heavily rely on the logical address and routing, which are vulnerable to the high satellite mobility earth’s rotations in reality. Therefore, a stable space-ground network at scale calls for a coherent design between cyberspace and reality.

We propose F-Rosette, a stable space-ground network structure in LEO mega-constellation. F-Rosette stabilizes the space-ground network in the virtual cyberspace by aligning it with the dynamic mega-constellations in the physical world. With the Rosette constellation as the basic building block, F-Rosette recursively constructs a provably stable network topology with inter-satellite links. On top of this stable network topology, we derive a hierarchical network address space for the satellites and terrestrial users. To prevent frequent address changes, we decouple this address space from mobility in F-Rosette’s new geographical coordinate system. Routing with F-Rosette’s network address is stable and efficient *without* requiring routing re-convergence, thus

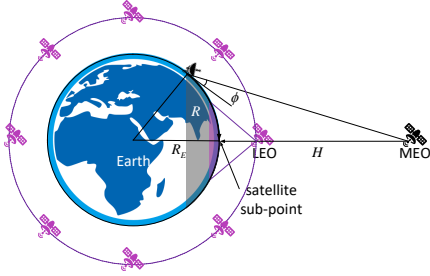


Figure 1: Satellites, constellations, and their coverages.

	Num. satellites	Num. orbits	Altitude H (km)	Inclination angle ϕ	Ground-to-space RTT (ms)
Starlink [1]	1584/1584/ 720/348/172	72/72/ 36/6/4	550/540/ 570/560/560	53/53/ 70/97/97	3.7/3.6/ 3.8/3.7/3.7
Kuiper [2]	1156/1296/784	34/36/28	630/610/590	52/42/33	4.2/4.07/3.93
Telesat [3]	351/1320	27/40	1015/1325	98.98/50.88	6.77/8.83
Iridium [9]	66	6	725	86.4	4.83

Table 1: Statistics of common LEO constellations.

retaining high network usability. Routing between satellites follows the standard IPv6 prefix/wildcard matching with provable optimality and multi-path support. To route traffic between terrestrial users, F-Rosette performs local geographical routing by embedding it into the topological routing between satellites over the stable network topology. For practical deployment, F-Rosette is backward compatible with IPv6, supports incremental expansion, and facilitates inter-networking to external networks.

We prototype F-Rosette’s protocol suite and evaluate it with hardware-in-the-loop, trace-driven emulations. Compared to existing mega-constellations, F-Rosette stabilizes network topology, addressing, and routing with near-optimal data delivery ($\leq 1.4\%$ additional delay). F-Rosette incurs negligible CPU ($< 1\%$) and memory ($< 2\text{MB}$) cost that is comparable to standard IPv6, thus suitable for small LEO satellites.

2 SPACE-GROUND NETWORK PRIMER

This section introduces the LEO satellite mega-constellations today (§2.1), and analyzes why they cannot guarantee stable space-ground network services (§2.2).

2.1 Satellites and Mega-Constellations

Satellites can be classified by their orbits’ altitude. A satellite can operate at low-earth orbit (LEO, $\leq 2,000$ km), medium-earth orbit (MEO, $\leq 35,786$ km), or high-earth orbit (HEO, $> 35,786$ km). An orbit can be described by its altitude, inclination to Equator, and right ascension angle¹. Traditional communication satellites usually operate at MEO orbits, such as the geostationary orbit (GEO, 35,786 km). As shown in Figure 1, a higher-altitude satellite offers larger coverage (defined as its great circle range R on the earth) but at the cost of longer ground-to-space round-trip latency.

¹In theory, 7 parameters are required to describe an orbit [10]. But real constellations need fewer degrees, e.g., circular orbit with zero eccentricity and same apogee/perigee. So we will use a simpler version in this paper.

A small LEO satellite usually has very limited coverage, computation power, and storage. To enable ubiquitous network services, one possible solution is to deploy an LEO *mega-constellation*. Table 1 summarizes the statistics of common mega-constellations today. The massive satellites help fully cover the areas of interest, while the LEO orbits ensure low ground-to-space round trips. Each satellite uses its microwave radio link for data transfer from/to terrestrial users. Satellites can interconnect with each other via free-space laser inter-satellite links. Unlike the traditional communications satellites at link layer only, LEO satellites in the mega-constellations should route traffic at the network layer and inter-connect to other terrestrial networks (e.g., via TCP/IP) for *global* Internet services *at scale* (acknowledged by Elon Musk [11] and recent work [12, 13]).

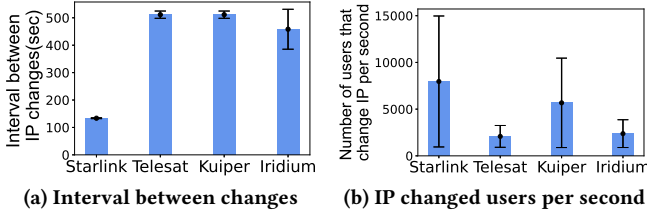
2.2 Unstable Space-Ground Network Today

The LEO mega-constellations aim to enable usable and performant network services for terrestrial users. Unfortunately, our analysis and trace-driven emulation project that, with the *dynamic many-to-many* space-ground mapping in high mobility, existing mega-constellations running standard IP will suffer from frequent IP address changes for the users and routing re-convergence for the network (thus low usability).

Why unstable: Dynamic many-to-many mapping In LEO mega-constellations, the many-to-many mapping between satellites and terrestrial users is a norm rather than an exception. Each LEO satellite can cover many users ($\approx 100,000$), while each terrestrial user has visibility to many satellites (≈ 20) in mega-constellations. This many-to-many mapping is dynamic due to high mobility. Compared to the MEO/GEO satellites, LEO satellites at a much lower altitude (typically $\leq 2,000$ km) exhibit high mobility² and relative motions. Moreover, terrestrial users also exhibit relative motions to the satellites due to the earth’s rotations. Both result in frequent changes of the network topology between space and ground.

How (un)stable is the space-ground network: We next quantify the impact of dynamic many-to-many mapping on the stability of the space-ground network. Since the LEO mega-constellations are still at their early deployments, their network designs are still underway and unfinished [5–7]. To this end, we conduct a trace-driven projection based on the operational mega-constellations in Table 1 over IPv6 in a hardware-in-the-loop emulator (detailed in §7). We consider two usage modes: (1) *Direct access*: A terrestrial user with a satellite phone directly accesses the satellite network. We follow the world population statistics from NASA in 2020 [14] and Starlink’s estimated customer numbers in the U.S. [15] to proportionally estimate the users that directly access

²According to Kepler’s third law, for all satellites of the earth, the ratio between their orbital altitude and period $(R_E + H_s)^3 / T_s^2$ is a constant.



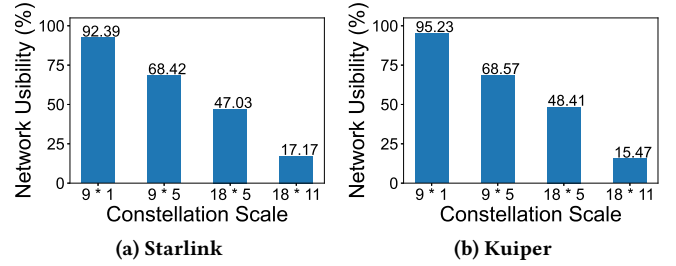
(a) Interval between changes (b) IP changed users per second
Figure 2: Projected users' IP address change frequency in LEO mega-constellations in the direct access mode.

satellite network at different locations. (2) *Ground station-assisted access*: Terrestrial users associate to a ground station [16, 17], which connects to a satellite for network access. We assume six ground stations in New York, Tokyo, Beijing, Hong Kong, Shanghai, and Singapore; the results for ground stations at other locations are similar. We assume each user or ground station will always associate to the physically nearest satellite for good coverage [18]. All network nodes run the IPv6 stack and OSPF. Figure 2 and Figure 3 show the projected impact on the users and the network, respectively.

◦ *Impact on users: Frequent IP address changes*. In the direct access mode, a terrestrial user's IP address belongs to the subnet of the corresponding satellite logical network interface. With rapid satellite motions, the terrestrial user has to frequently handoff to new satellites (thus new network interfaces and addresses) to retain its Internet access. As shown in Figure 2, each user is forced to change its logical IP address every 133–510s, and every second we observe 2082–7961 global users per second should change their IP addresses. Such frequent address changes will repetitively disrupt the TCP connections and upper-layer applications, and will negatively impact the user experiences.

◦ *Impact on network: Frequent routing re-convergence and low usability*. To prevent frequent user IP changes, one can adopt the ground station-assisted access mode. In this mode, the ground station is a gateway for a fixed IP subnet, so that all users associating with it retain the time-invariant address. As the ground station re-associates to a new satellite, the space-ground logical network topology changes. Then the IP routing must re-converge to guarantee reachability to this ground station, before which the network cannot route traffic to the ground station. Note each LEO satellite can only provide very short coverage for a ground station (10 minutes in Iridium, ≤ 3 minutes in Starlink). Frequent handoffs between satellites result in repetitive routing re-convergence and thus low network usability (i.e., $1 - \frac{\text{routing re-convergence duration}}{\text{each satellite's service duration}}$). Figure 3 shows that, all mega-constellations today suffer from $\leq 20\%$ network usability even under small constellations. The network usability decreases with more satellites, which causes more frequent handoffs for ground stations.

How mega-constellation amplifies instability: Both issues will worsen with more satellites in the mega-constellations.



(a) Starlink (b) Kuiper
Figure 3: Projected network usability in LEO mega-constellations in ground station-assisted mode.

Users in the direct access mode will experience more hand-offs with more satellites, thus causing more frequent IP address changes. For the network in the ground station-assisted mode, Figure 3 shows more satellites prolong the routing re-convergence on link change, thus lowering the network usability. Moreover, more satellites complicate the dynamic routing between the moving satellites and terrestrial users (due to the earth's rotation). Solutions for small LEO networks decades ago (e.g., virtual topology [19, 20] and virtual nodes [21, 22]) cannot scale to the mega-constellations today due to their vulnerability to dynamic many-to-many mapping, and expensive (pre-)computation and storage for small LEO satellites. Motivated by this, we next design *F-Rosette*, a stable space-ground network structure for LEO mega-constellations.

3 THE F-ROSETTE NETWORK STRUCTURE

We introduce *F-Rosette*'s structure and its basic properties.

3.1 A Primer of Rosette Constellation

The basic building block of *F-Rosette* is a Rosette constellation, which was originally proposed in [23] to guarantee full coverage with as few satellites as possible. This section introduces the necessary background of Rosette constellation for *F-Rosette*; a complete description is available in [23].

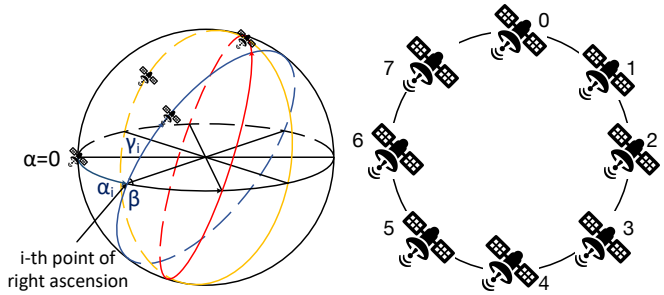
Figure 4 exemplifies the Rosette constellation with 8 satellites. Each orbit has one satellite, and all satellites move in circular orbits at the altitude of H (thus period T). A Rosette constellation is defined as a tuple (N, m) , where N is the number of satellites and $m \in \mathbb{N}$ is a harmonic phase shift. All satellites are numbered from 0 to $N - 1$. For satellite i , its runtime location can be described by three constant angles $(\alpha_i, \beta_i, \gamma_i)$ and one time-varying phase angle x_t at time t :

$$\alpha_i = \frac{2\pi i}{N}, i = 0, 1, \dots, N - 1 \quad (1)$$

$$\beta_i \equiv \beta, \forall i \quad (2)$$

$$\gamma_i = m\alpha_i = m \cdot \frac{2\pi i}{N} \quad (3)$$

$$x_t = \frac{2\pi}{T_s} t \quad (4)$$



(a) Physical constellation in space (b) Logical topology in F-Rosette₀
Figure 4: A Rosette constellation with $N = 8, m = 6$.

where α_i is satellite i 's right ascension angle, $\beta_i \equiv \beta$ is the inclination angle for all orbits, γ_i is i 's initial phase angle in its orbit at time $t = 0$, and x_t is the time-varying phase angle (*identical for all satellites anytime*). Compared to other constellations, the Rosette constellation has two appealing properties for networking:

Full coverage with fewer satellites: The Rosette constellation usually needs fewer satellites than Walker (building block for Starlink and Kuiper) and polar orbits for full coverage (see [23] and §7.1 for the evaluations). Each satellite's coverage R in Figure 1 can be determined by its altitude H and elevation angle ϕ :

$$\tan \phi = \frac{\cos R - R_E / (R_E + H)}{\sin R} \quad (5)$$

For LEO satellites, given each satellite's coverage R on the earth, the minimum number of satellites N_{min} needed to fully cover the earth is decided by the following relation:

$$\sec R = \sqrt{3} \tan \left(\frac{\pi}{6} \frac{N_{min}}{N_{min} - 2} \right) \quad (6)$$

Periodic ground-track repeat orbits: Due to the earth rotation and high LEO satellite mobility, the satellite sub-point in Figure 1 is time-varying and non-repeatable in general³ (exemplified in Figure 10). This complicates locating and routing between the ground and space. Instead, the Rosette constellation allows LEO satellites to retain periodic satellite sub-points via ground-track repeat orbits, i.e., every satellite will *periodically* revisit its previous satellite sub-point. To do so, we configure the satellites' orbital period T_s such that

$$T = T_E / (N - m) \quad (7)$$

where T_E is the period of earth rotation. For each satellite i , the latitude φ_i and longitude λ_i of its sub-point is:

$$\sin \varphi_i = \sin \beta \sin m(\omega_E t - \alpha_i) \quad (8)$$

$$\tan [\lambda_i + m(\omega_E t - \alpha_i)] = \cos \beta \tan m(\omega_E t - \alpha_i) \quad (9)$$

where $\omega_E = 2\pi/T_E$ is the earth's angular rotation speed.

Despite these merits, however, the original Rosette constellation is not immediately applicable to networking. It was

³The geostationary satellites guarantee time-invariant satellite sub-point, but at the altitude of 35,786km and thus suffer from long network latency.

Algorithm 1 F-Rosette construction.

Input: A Rosette constellation (N, N, m) , and a F-Rosette level $k \geq 0$
Output: F-Rosette _{k}
1: F-Rosette₀ = (N, N, m) Rosette constellation;
2: **for** $j=1$ to k **do**
3: F-Rosette _{j} = {};
4: **for** $i=0$ to $N-1$ **do** ▷ Step 1: Construct N F-Rosette _{$j-1$} s
5: F-Rosette _{$j-1$} ^{i} = Shift(F-Rosette _{$j-1$} , $\frac{2\pi}{N}$);
6: F-Rosette _{j} .append(F-Rosette _{$j-1$} ^{i});
7: **end for**
8: **for** $i=0$ to $N-1$ **do** ▷ Step 2: Inter-connect F-Rosette _{$j-1$} s
9: **for** each satellite S_i in F-Rosette _{$j-1$} ^{i} **do**
10: Connect S_i to $S_{(i+1 \bmod N)}$ in F-Rosette _{$j-1$} ^{$(i+1 \bmod N)$} ;
11: **end for**
12: **end for**
13: **end for**
14: **return** F-Rosette _{k} ;

primarily designed for full coverage rather than network routing. There was no specification on how to inter-connect satellites, how to forward traffic among satellites, and how to route data among terrestrial users via satellites. This motivates us to re-struct the Rosette constellation for stable space-ground network at scale.

3.2 F-Rosette Construction

F-Rosette adopts the Rosette constellation as a base case, but extends it recursively with inter-satellite links. Specifically, a F-Rosette₀ is a (N, m) Rosette constellation in §3.1, with inter-satellite links in adjacent satellites (exemplified in Figure 4b) and ground-track repeat orbits for all satellites. A F-Rosette _{k} ($k \geq 1$) is constructed recursively from N F-Rosette _{$k-1$} s. Algorithm 1 shows F-Rosette construction. It takes two phases (exemplified in Figure 5):

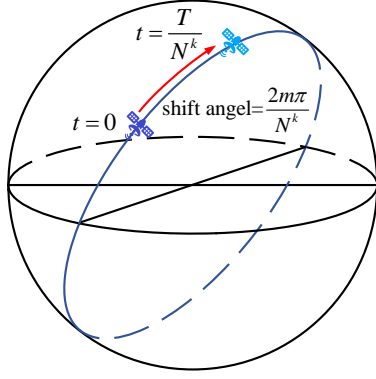
(1) Construct N F-Rosette _{$k-1$} s: The F-Rosette _{$k-1$} s are numbered from 0 to $N-1$ as F-Rosette _{$k-1$} ⁰, F-Rosette _{$k-1$} ¹, ..., F-Rosette _{$k-1$} ^{$N-1$} . As shown in Figure 5a, F-Rosette _{$k-1$} ^{i} is obtained by first duplicating a F-Rosette _{$k-1$} ⁰, and then shifting it by a time interval $t_k = \frac{T_s}{N^k}$ (or equivalently a phase angle shift $x_k = \frac{2\pi}{T_s} \cdot t_k = \frac{2\pi}{N^k}$ according to Equation 4). Each satellite S_j in F-Rosette _{$k-1$} ⁰ is replicated N times on the same orbit, denoted as $S_j^0, S_j^1, \dots, S_j^{N-1}$.

(2) Interconnect F-Rosette _{$k-1$} s: The next step is to bridge F-Rosette _{$k-1$} s with *intra-orbit* inter-satellite links only. As shown in Figure 5b and Figure 5c, each S_i in F-Rosette _{$k-1$} ^{i} ($i = 0, 1, \dots, N-1$) adds a link to $S_{(i+1 \bmod N)}$ in F-Rosette _{$k-1$} ^{$(i+1 \bmod N)$} . This creates a circle among satellites on the same orbit.

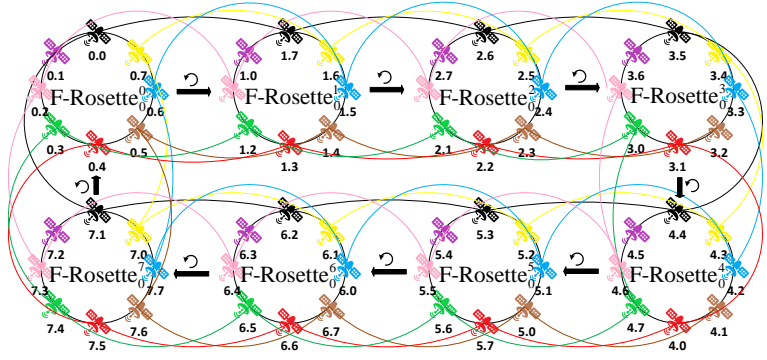
3.3 Basic Properties of F-Rosette

F-Rosette inherits all good properties from the classical Rosette constellation in §3.1, and has additional appealing features for networking due to its recursive architecture.

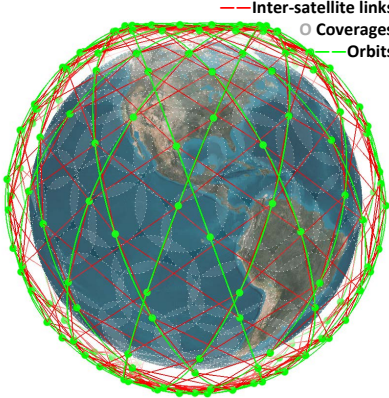
Network structure size: A F-Rosette _{k} has N^{k+1} satellites and $(k+1)N^{k+1}$ inter-satellite links. Table 2 exemplifies



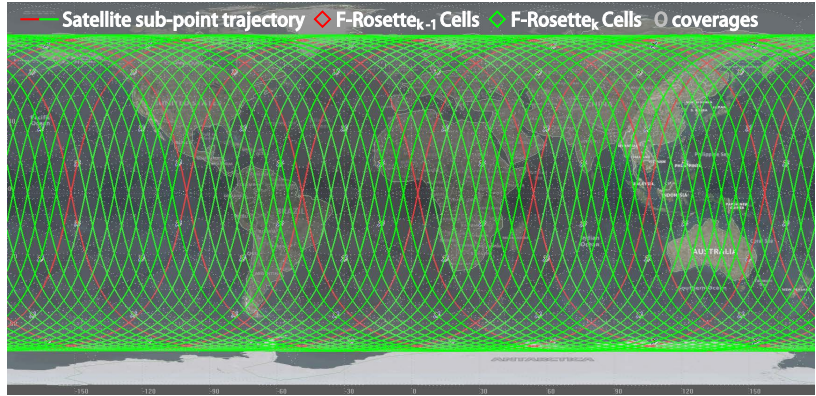
(a) Shift(F-Rosette, t) in Algorithm 1



(b) Logical network topology of F-Rosette_k



(c) Physical constellation in 3D space



(d) Hierarchical geographical cells by fixed satellite sub-point trajectories.

Figure 5: Recursive construction of F-Rosette.

the scale when $N = 8$. Each satellite has $2(k+1)$ inter-satellite links, which is affordable even for small LEO satellites (typically 4–5 links [12, 13]).

Full coverage: Each F-Rosette_k is also a Rosette constellation and thus can ensure full coverage. Specifically, we have the following theorem (proved in Appendix A):

Theorem 1 (Full coverage). *A F-Rosette_k guarantees full coverage if its satellites' altitude $H > H_{min}$, where*

$$H_{min} = R_E \left(\frac{1}{\cos R - \sin R \tan \phi} - 1 \right)$$

$$R = \sec^{-1} \left(\sqrt{3} \tan \left(\frac{\pi}{6} \frac{N^{k+1}}{N^{k+1} - 2} \right) \right)$$

With this full coverage guarantee, a satellite operator can customize the F-Rosette size to meet its demands. In Appendix B, we show how to select the size given the demand of ground-to-space RTT and the minimum elevation angle.

Stable network topology: F-Rosette guarantees time-invariant network topology despite satellites' high mobility and earth's rotation. This is desirable to simplify the routing and ensure high network usability (§2.2). F-Rosette guarantees the logical connection between any two satellites remains always-on and unchanged. This can be achieved by

Table 2: F-Rosette's satellites' altitude with $N=8/16$, $m=1$, and the elevation angle $\phi = 25^\circ$.

		Num. satellites	Minimum altitude (km)	Ground-to-space RTT (ms)	Avg. cell size (km ²)
∞	F-Rosette ₀	8	11848.46	78.99	9,060,419
	F-Rosette ₁	64	1259.58	8.40	141,569
	F-Rosette ₂	512	335.33	2.23	2,212
16	F-Rosette ₀	16	4268.73	28.46	1,973,158
	F-Rosette ₁	256	504.83	3.36	7,707
	F-Rosette ₂	4096	107.62	0.72	30

specifying the minimum altitude of all satellites, as shown below (proved in Appendix C):

Theorem 2 (Stable network topology). *The network topology of a F-Rosette_k remains stable if its satellites' altitude $H > \max\{(\frac{1}{\cos \frac{r_{max}}{2}} - 1)R_E, H_{min}\}$, where r_{max} is the max great circle range of inter-orbit links and R_E is the earth radius.*

Stable satellite sub-point trajectory: F-Rosette always adopts the Rosette constellations with ground-track repeat orbits $T = T_E / (N - m)$. As shown in Figure 5d, this results in stable and periodic satellite sub-point trajectory. As we will see in §4, these trajectories enable hierarchical space-ground network addresses and simplify routing.

Propagation delay of an inter-satellite link: Despite high satellite mobility, F-Rosette retains *regular and predictable* delay variations for each inter-satellite link. For intra-orbit links, F-Rosette guarantees *fixed* propagation delay

between two satellites, due to their time-invariant distances. For the inter-orbit links, its length (thus propagation delay) unavoidably varies over time. For any two satellites i and j in different orbits, its inter-satellite link length L_{ij} and propagation delay τ_{ij} :

$$L_{ij}(t) = 2(H + R_E) \sin(r_{ij}(t)/2) \quad (10)$$

$$\tau_{ij}(t) = L_{ij}(t)/c \quad (11)$$

where $r_{ij}(t)$ is the *range* between i and j on the great circle:

$$\begin{aligned} \sin^2(r_{ij}(t)/2) &= \cos^4(\beta/2) \sin^2(m+1)(j-i)(\pi/N) \\ &+ 2 \sin^2(\beta/2) \cos^2(\beta/2) \sin^2 m(j-i)(\pi/N) \\ &+ \sin^4(\beta/2) \sin^2(m-1)(j-i)(\pi/N) \\ &+ 2 \sin^2(\beta/2) \cos^2(\beta/2) \sin^2(j-i)(\pi/N) \\ &\cdot \cos\left[\frac{4\pi}{T}t + 2m(j+i)(\pi/N)\right] \end{aligned} \quad (12)$$

Note such delay is *periodic* and *bounded*, thus facilitating delay-sensitive apps. We will evaluate the link delay in §7.1.

4 NETWORK ADDRESSING IN F-ROSETTE

We next define F-Rosette's hierarchical network addressing for space and ground. We show how F-Rosette decouples its network addressing from mobility for stability, and avoids frequent user IP changes in §2.2.

4.1 Hierarchical Addressing for Satellites

F-Rosette's recursive structure naturally defines hierarchical network addresses for its satellites. We assign each satellite S in F-Rosette $_k$ with a hierarchical address $s_0.s_1.s_2\dots s_k$ ($s_i = 0, 1, \dots, N-1, \forall i$). Each digit s_i represents the corresponding F-Rosette $_i$ structure that S belongs to. The length of this satellite address is $k \log N$ bits (which is usually small as evaluated in §7.2). This hierarchical address can be naturally embedded into IPv6's address space, as shown in Figure 7a. It is constant despite satellite mobility, since it only relies on F-Rosette's stable network topology.

4.2 Hierarchical Addressing for Ground

To stabilize the addressing in high mobility, F-Rosette divides the earth's spherical surface into a hierarchy of disjoint *geographical cells* and allocates cell-based addresses to terrestrial users and ground stations. In this way, the network addresses are decoupled from the satellite and earth mobility, thus free of frequent changes (§2.2). They are unchanged unless the users move to a new geographical cell. Figure 5d exemplifies F-Rosette's cells. Each cell is a quadrilateral bounded by four satellite sub-point trajectories of

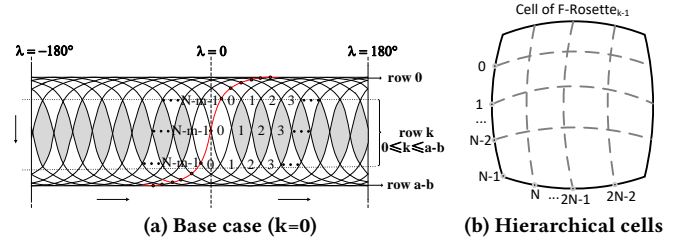


Figure 6: Hierarchical geographical cells in F-Rosette.

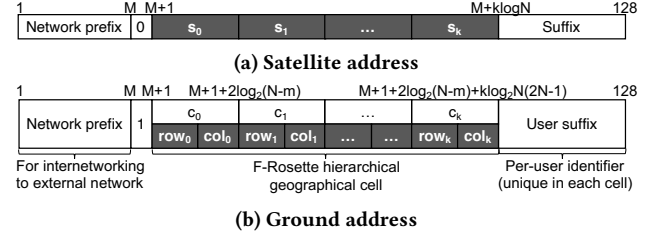


Figure 7: Embedding F-Rosette into IPv6 address.

F-Rosette's satellites. The F-Rosette cells exhibit three appealing features for satellite routing in space:

Stable geographical cells: F-Rosette's satellites run on the ground-track orbits (§3.2), which implies all satellite sub-point trajectories are *time-invariant*. Therefore, despite the high satellite mobility and earth's rotation, each F-Rosette cells's location, size, and coverage are fixed and invariant.

Hierarchical geographical cells: F-Rosette's recursive and symmetric structure forms a hierarchy of cells. With recursive construction, each cell in the F-Rosette $_{k-1}$ will be divided into a group of sub-cells in F-Rosette $_k$. This hierarchy is exemplified in Figure 6b and validated by the following theorem (proved in Appendix D):

Theorem 3 (Hierarchical geographical cells). *When constructing F-Rosette $_k$ from F-Rosette $_{k-1}$, each geographical cell in F-Rosette $_{k-1}$ will be divided into N^2 disjoint sub-cells in F-Rosette $_k$.*

We also have the total number of cells in a F-Rosette $_k$ as follows (proved in Appendix F):

Lemma 1. A F-Rosette $_k$ divides its coverage areas into $(N-m)^2 N^{2k}$ disjoint cells.

Network addressing for the ground: F-Rosette assigns geographical address to each ground user based on the cell it resides. Figure 7b illustrates how this geographical cell ID can be readily realized embedded into IPv6⁴. For each user in this cell, F-Rosette assigns its address as a concatenation of new prefix, hierarchical geographical ID, and the user suffix. The network prefix is used for inter-networking with external networks and backward compatibility with standard IPv6 (§6). The per-user suffix guarantees the globally unique address inside each geographical cell. In this way, the user address remains *invariant* unless (s)he moves to a

⁴Besides IPv6, this address can also be embedded into the future architecture such as NDN [24, 25], SCION [26], MobilityFirst [27], and XIA [28].

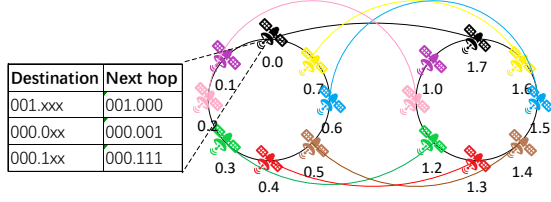


Figure 8: Prefix/wildcard match in F-Rosette routing.

new cell (which is rare due to the cell size in Table 2). To help detect if the address is for satellite or ground for routing in §5, we add a 1-bit flag to differentiate their addresses.

We next elaborate on how to allocate the hierarchical geographical cell IDs. A geographical cell in $F\text{-Rosette}_k$ is uniquely identified by $c_0.c_1\dots.c_k$, where $c_0 = 0, 1, \dots, (N - m)^2 - 1$ and $c_i = 0, 1, \dots, N^2 - 1 (i \neq 0)$. Each digit c_i represents the corresponding $F\text{-Rosette}_i$ cell identifier that this user belongs to, and can be further decomposed into a row ID row_i and column ID col_i . For $F\text{-Rosette}_0$, its sub-satellite point trajectories and two latitude lines divide the earth into $N - m$ row and $N - m$ columns, and we identify each cell with the left point. As shown in Figure 6a, we number each row from 0 to $N - m - 1$ from north to south. Starting from the cell whose left dot is on the trajectory of satellite 0 above the equator and its extension line, each column is numbered from 0 to $N - m - 1$ according to the increasing direction of the longitude value. Next, a $F\text{-Rosette}_k (k \geq 1)$ divides each cell in $F\text{-Rosette}_{k-1} (k \geq 1)$ into $2N - 1$ layers. We number each layer from 0 to $2N - 2$ in the direction from north to south, and at the same time, we number cells in each layer from left to right. Encoding this hierarchical geographical cell address requires $2k \log N + 2 \log[(N - m)]$ bits (which is usually small for IPv6, as evaluated in §7.2).

5 ROUTING IN F-ROSETTE

We describe how F-Rosette enables stable, highly-usable, and efficient routing without re-convergence (§2.2). We first show how to route between satellites over F-Rosette’s stable graphical topology (§5.1). Then we show how to route between ground users by embedding hierarchical geographical routing into the satellites’ topological routing (§5.2).

5.1 Topological Routing for the Satellites

With its stable and regular constellation, F-Rosette supports efficient and highly-usable single/multi-path routing that is compatible with standard Internet routing mechanisms.

Single-path routing: With F-Rosette’s regular topology, a satellite can *locally* compute the shortest path without global routing (re-)convergence and thus avoids low network usability in §2.2. Algorithm 2 shows the shortest-path routing from a source satellite $S=s_0.s_1.s_2\dots.s_k$ to a destination $D=d_0.d_1.d_2\dots.d_k$ defined in §4.1. A pre-defined permutation

Algorithm 2 Shortest-path satellite routing in F-Rosette.

Input: Source satellite address $S=s_0.s_1.s_2\dots.s_k$, destination satellite address $D=d_0.d_1.d_2\dots.d_k$, and a permutation $P = [p_0, p_1, \dots, p_k]$ of $[0, 1, \dots, k]$

Output: A path from S to D

```

1: path(S,D)={S}; next_hop=S;
2: for i=p_0, p_1, ..., p_k do           ▷ The permutation shuffles indexes for multi-path routing
3:   if next_hop[i] - d_i mod N ≤ N/2 then   ▷ Clockwise routing is shorter
4:     while next_hop[i] ≠ d_i do
5:       next_hop[i] = next_hop[i]+1 mod N;
6:       path(S,D).append(next_hop);
7:     end while
8:   else                                     ▷ Counter-clockwise routing is shorter
9:     while next_hop[i] ≠ d_i do
10:      next_hop[i] = next_hop[i]-1 mod N;
11:      path(S,D).append(next_hop);
12:    end while
13:   end if
14: end for
15: return path;
```

$P = [p_0, p_1, \dots, p_k]$ of indexes $0, 1, \dots, k$ is also given as an input to facilitate the enumeration of multiple paths (detailed below). To route traffic from S to D , we follow the permutation P to traverse all layers of $F\text{-Rosette}_k$. At each layer p_i , all satellites form a ring topology according to §3.2. The shortest path is either the clockwise or counter-clockwise routing. To find the shortest path, we first decide the routing direction, and then increment (or decrement) the p_i -th digit of the previous satellite’s address, until the p_i -th digit equals the destination’s corresponding digit d_{p_i} . The correctness of Algorithm 2 is therefore straightforward:

Theorem 4 (Shortest path). *Algorithm 2 finds the shortest path in hop counts between any two satellites.*

F-Rosette’s routing exhibits three desirable features:

(1) *Stable and highly usable without re-convergence:* Algorithm 2 avoids global routing (re-)convergence in F-Rosette’s regular and stable topology, thus retain high usability despite dynamic many-to-many mapping (§2.2). With F-Rosette’s regular structure, the satellite’s address inherently implies the routing path. Each satellite can locally decide the next hop without global routing (re-)convergence.

(2) *Prefix/wildcard-based routing table:* With F-Rosette’s hierarchical satellite address, Algorithm 2 can be realized with the standard prefix/wildcard matching in IP networks. Figure 8 exemplifies the routing table for Algorithm 2. With the ring topology at each F-Rosette layer, destinations with the same prefix (or layer) can be aggregated as a single entry in the standard routing table. The storage required by the F-Rosette routing table is also small for memory-constrained satellites (proved in Appendix E):

Theorem 5 (FIB storage bound). *Each satellite in a $F\text{-Rosette}_k$ has at most $2(k + 1) \lceil \log \frac{N}{2} \rceil$ entries in its routing table.*

(3) *Performance bound:* F-Rosette’s regular structure also provides bounded latency for its single-path routing. The upper bound can be derived from Algorithm 2 as follows:

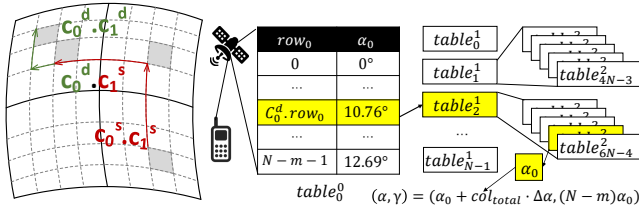


Figure 9: Hierarchical geographical routing for users.

Theorem 6 (Hop bound). *The maximum number of hops between two satellites in F-Rosette_k is no more than $\frac{(k+1)N}{2}$.*

Multi-paths: F-Rosette also offers abundant parallel paths for performance acceleration and fault tolerance. By enumerating the permutations P of the F-Rosette layers $[0, 1, \dots, k]$, Algorithm 2 yields parallel paths from the same source-destination pair. The following theorem shows the available paths in F-Rosette (proved in Appendix G):

Theorem 7 (Multi-path). *There are $2(k+1)$ disjoint parallel paths between any two satellites in a F-Rosette_k.*

Stability and high network usability: With its stable network topology, F-Rosette ensures stable routing despite high mobility. Each satellite locally routes traffic without requiring slow global (re-)convergence. This prevents the low network usability as discussed in §2.2.

5.2 Geographical Routing for the Ground

F-Rosette adopts geographical routing to deliver traffic between terrestrial users. Geographical routing is appealing for its efficiency, scalability, and high network usability. It takes the physically short path to forward the traffic. Moreover, geographical routing can be mostly performed locally without global routing (re-)convergence, thus avoiding low network usability in mobility (§2.2).

F-Rosette supports native *hierarchical* geographical routing for the ground. As shown in Figure 9, data from cell $c_0^s, c_1^s, \dots, c_k^s$ to $c_0^d, c_1^d, \dots, c_k^d$ in §4.2 can traverse from c_i^s to c_i^d at each level i of the F-Rosette cells. In F-Rosette, this geographical routing can be converted to an equivalent topological routing between satellites in §5.1, thus retaining stability and efficiency. We next elaborate on it.

Space-ground alignment with F-Rosette coordinates:

The first step for F-Rosette’s geographical routing is to align the logical satellite address in the cyberspace and ground locations in the physical world. F-Rosette’s structure implies a geographic coordinate system that facilitates this. Figure 4a exemplifies this coordinate system. Different from the classical Cartesian coordinates or latitudes/longitudes, F-Rosette defines the position of each location on the earth as (α, γ) , where α is its right ascension angle, and γ is the phase angle along a virtual orbit of inclination β across the right ascension angle. This coordinate aligns the ground location with F-Rosette’s satellite sub-point trajectories, thus

Algorithm 3 F-Rosette’s geographical routing for ground.

Input: Source user’s serving satellite’s $S = (\alpha_s(t), \gamma_s(t))$ and destination user’s cell $D = (\alpha_d, \gamma_d)$

Output: A routing path from S to D through F-Rosette satellites

```

1: path(S,D)={S}; next_hop=S;
2:  $\Delta\alpha = \alpha_d - \alpha_s(t) \bmod 2\pi$ ;  $\Delta\gamma = \gamma_d - \gamma_s(t) \bmod 2\pi$ ;
3: if  $\Delta\alpha < \pi$  then ▷ Clockwise routing is shorter
4:   while  $\Delta\alpha \geq \frac{2\pi}{N}$  do
5:     next_hop[0] = next_hop[0]+1 mod N;
6:      $\Delta\alpha = \Delta\alpha - \frac{2\pi}{N} \bmod 2\pi$ ;  $\Delta\gamma = \Delta\gamma - \frac{2m\pi}{N} \bmod 2\pi$ ;
7:     path(S,D).append(next_hop); goto Line 31 if next_hop covers D;
8:   end while
9: else ▷ Counter-clockwise routing is shorter
10:  while  $\Delta\alpha \geq \frac{2\pi}{N}$  do
11:    next_hop[0] = next_hop[0]-1 mod N;
12:     $\Delta\alpha = \Delta\alpha + \frac{2\pi}{N} \bmod 2\pi$ ;  $\Delta\gamma = \Delta\gamma + \frac{2m\pi}{N} \bmod 2\pi$ ;
13:    path(S,D).append(next_hop); goto Line 31 if next_hop covers D;
14:  end while
15: end if
16: for  $i=1, 2, \dots, k-1$  do
17:   if  $\Delta\gamma < \pi$  then ▷ Clockwise routing is shorter
18:   while  $\Delta\gamma \geq \frac{2m\pi}{N^k}$  do
19:     next_hop[i] = next_hop[i]+1 mod N;
20:      $\Delta\gamma = \Delta\gamma - \frac{2m\pi}{N^k} \bmod 2\pi$ ;
21:     path(S,D).append(next_hop); goto Line 31 if next_hop covers D;
22:   end while
23: else ▷ Counter-clockwise routing is shorter
24:   while  $\Delta\gamma \geq \frac{2m\pi}{N^k}$  do
25:     next_hop[i] = next_hop[i]-1 mod N;
26:      $\Delta\gamma = \Delta\gamma + \frac{2m\pi}{N^k} \bmod 2\pi$ ;
27:     path(S,D).append(next_hop); goto Line 31 if next_hop covers D;
28:   end while
29: end if
30: end for
31: return path;
```

facilitating the geographical-to-topological routing below. In this coordinate, each satellite’s sub-point location (α, γ) can be mapped to the runtime latitude φ and longitude λ as follows (derived from Equation 1, 3, 8, and 9):

$$\sin \varphi = \sin \beta \sin (N\omega_{Et} - \gamma)$$

$$\tan (\lambda + \omega_{Et} - \alpha) = \cos \beta \tan (N\omega_{Et} - \gamma)$$

Due to the high mobility, a satellite sub-point’s longitude shifts over time with dynamic mapping between (α, γ) and (φ, λ) . Despite so, it is easy to verify from Equation 1–4 that, the *relative position* $(\Delta\alpha, \Delta\gamma)$ between any two connected satellites’ sub-points remains *constant*. This results in an important property to bridge the topological routing between satellites and geographical routing between ground cells:

Property 1 (Space-ground routing alignment). *A packet routed through an inter-orbit satellite link in F-Rosette moves a fixed relative position of*

$$\Delta\alpha_0 = \frac{2\pi}{N}, \Delta\gamma_0 = \frac{2\pi m}{N}$$

A packet routed through an intra-orbit satellite link at layer $j = 1, 2, \dots, k$ moves a fixed relative position of

$$\Delta\alpha_j = 0, \Delta\gamma_j = \frac{2\pi m}{N^k}$$

Geographical-to-topological routing embedding: Property 1 implies routing between satellites in Algorithm 2 is equivalent to traversing a *fixed* relative position in F-Rosette’s coordinate system. Given two cells $S = c_0^s.c_1^s\dots.c_k^s$ and $D = c_0^d.c_1^d\dots.c_k^d$, one can compute their relative position $(\Delta\alpha, \Delta\gamma)$ via table lookup (detailed below), and route the traffic from S to D by following the topological routing in Algorithm 2 to hierarchically shorten the packet’s relative position to D . This is equivalent to the geographical routing in Figure 9.

Algorithm 3 elaborates on the geographical ground routing via topological satellite routing. It extends Algorithm 2, and maps the relative motion to hop count. It uses the source user’s serving satellite’s sub-point as the input, which is locally maintained by the satellite as $\alpha_s(t) = \alpha_s(0) - \frac{2\pi}{T_E}t$, $\gamma_s(t) = \gamma_s(0) + \frac{2\pi}{T}t$ (Equation 1–4). The routing ends if the user in target cell is covered by the current satellite (detected if the current satellite finds the user associates to it at the link layer). Algorithm 3 can be realized atop Algorithm 2, thus retaining high efficiency for resource-constrained satellites.

Avoiding local minimum and last-hop ambiguity: A classical problem for the greedy geographical routing is the local minimum [29–32], i.e., the physically nearest satellite is not reachable for delivery (mostly due to limited coverage). This problem is largely mitigated in F-Rosette: Similar to greedy embedding [33, 34], geographical routing in Algorithm 3 relies on topological routing in §5.1 for guaranteed reachability and successful delivery. The only exception is the last hop, where the terrestrial user does not associate to the nearest satellite. Since the ground-satellite link depends on user-specific satellite selection strategy and is beyond the satellite topology, simply relying on topological routing is insufficient to guarantee delivery. Fortunately, Algorithm 3 over F-Rosette’s ring structure implies all satellites at each layer can be reached in the worst case. This ensures eventually the user-selected satellite will be reached for successful delivery, at some cost of detouring delays.

Data forwarding acceleration via table lookup: Similar to the topological routing, geographical routing in Algorithm 3 can also be accelerated via table lookup at least four aspects. First, the relative motion between connected satellites $(\Delta\alpha_k, \Delta\gamma_k)$ can be pre-computed and pre-stored in each FIB entry, thus avoiding runtime per-packet computation in Algorithm 3. Second, to decide the destination cell’s location (α_d, γ_d) given its cell ID $c_0^d.c_1^d\dots.c_k^d$, each satellite can pre-compute and store a hierarchical lookup table as shown in Figure 9. Since all geographical cells are formed by the satellite sub-points, one can follow Equation 8–9 to pre-compute each cell’s location for hierarchical lookup. This results in a table with $\frac{(N-m)N^k}{2}$ entries and $O(k+1)$ runtime lookup time (elaborated in Appendix H). Third, to avoid repetitively

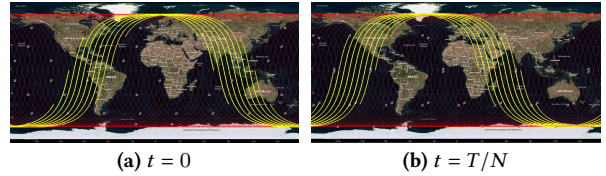


Figure 10: Exploiting regular satellite mobility to guarantee data delivery in flat incremental expansion.

computing the source user’s serving satellite’s runtime location $(\alpha_s(t), \gamma_s(t))$ for all packets, the satellite can cache its runtime location and refresh it every $\frac{T}{2N^k}$ seconds (which guarantees consistent forwarding decision given the minimal $(\Delta\alpha_k, \Delta\gamma_k)$). Last but not least, to avoid repetitive next-hop calculation for the packets to the same destination cell, a satellite can create a cached geographical FIB entry and periodically update it every $\frac{T}{2N^k}$ seconds.

Stability and high network usability: F-Rosette embeds geographical routing into F-Rosette’s stable network topology, thus facilitating stable routing. Similar to topological routing in §5.1, F-Rosette’s geographical routing relies on local information only. It does not require the slow routing (re)-convergence, thus retaining high network usability despite high satellite mobility and earth’s rotation (§2.2).

6 ISSUES IN PRACTICAL DEPLOYMENT

In this section, we discuss various issues and solutions for the deployment of F-Rosette in practice.

Incremental expansion: In practice, it is unlikely to deploy F-Rosette all at once. The satellites can only be launched to space incrementally. For example, as of January 2021, the latest SpaceX Falcon 9 rocket can launch up to 143 satellites each time [35], which is less than F-Rosette₁’s 256 satellites when $N = 16$. When incrementally expanding F-Rosette in space, it is desirable to retain always-on, seamless network services for existing users. This demand results in three concrete goals in expansion: (1) guarantee data delivery despite incomplete deployment; (2) avoid re-interconnection of satellites whenever possible; and (3) retain stable address during the deployment.

A straightforward way to incrementally deploy F-Rosette is to follow Algorithm 1, i.e., launch F-Rosette _{$k-1$} first and recursively expand it to F-Rosette _{k} . This ensures stable network topology and addresses, but can’t guarantee delivery with partial coverage *before* all satellites are launched (§3.2).

To this end, we propose an iterative incremental expansion scheme, and exploit regular satellite mobility to guarantee the data delivery. Instead of building F-Rosette _{k} from F-Rosette _{$k-1$} , we incrementally deploy it *orbit by orbit*. Following step 8–12 in Algorithm 1, each time we deploy satellites that uniformly distribute on the same orbit. As exemplified in Figure 10, F-Rosette satellites in the same orbit form a moving wave of satellite sub-point trajectories that traverse the entire coverage. This differs from the satellite sub-points in a complete F-Rosette _{$k-1$} , which are fixed and thus limit

its full coverage at lower altitude. As the satellite sub-point trajectories move, all users have the opportunity to send the data to the satellite sometime. If a packet’s destination is currently outside the coverage, it can be buffered by the satellite and eventually delivered if any one of the satellite on the same orbit covers the destination. With more satellites deployed, more packets will be delivered via routing and less packets will be buffered. Similar to DTN in classical satellite networking [36, 37], this approach is feasible when the F-Rosette users are all tolerant to data delays.

Implications for ground stations: The ground stations can play as “gateways” to bridge the satellite and terrestrial networks, or download telemetry data from satellites [16, 17, 38, 39]. It is desirable to deploy the ground stations where they can maximize its radio quality and access to more satellites. F-Rosette’s stable satellite-to-ground mapping offers a natural solution for this. A ground station using F-Rosette can be deployed at the intersection of the fixed satellite sub-point trajectories. This guarantees maximal received power from the satellites (right above the ground station), and helps gain visibility to more satellites.

Network address allocation: The satellites’ F-Rosette addresses in §4.1 are fixed and can be pre-allocated before they are launched. For the ground users, their F-Rosette addresses in §4.2 are fixed unless they move to a new geographical cell. To tackle it, a DHCP address server (e.g., at the ground station) can be deployed for each cell to manage the address allocation and duplication detection. As evidenced in Figure 7b, the DHCP server can generate a F-Rosette address by concatenating the network prefix, the geographical cell ID, and a per-user suffix that is unique inside this cell.

Inter-networking to external networks: The discussion so far focuses on the networking inside a F-Rosette. In reality, both the terrestrial users and satellites need to communicate with others through the Internet. For compatibility with Internet routing and global reachability, we propose IPv6-based network addressing for F-Rosette. As shown in §4 and exemplified in Figure 7, the IPv6 prefix in Figure 7b can be used to identify whether a packet is inside a F-Rosette. If so, the F-Rosette routing in §5 can be applied. Otherwise, the packet will leave F-Rosette and enter the external network. In this case, the classical prefix match-based IP routing will be applied to the IPv6 address, thus retaining backward compatibility and global reachability.

Stability-performance tradeoff: F-Rosette’s primary goal is stability for a usable space-ground network. It is possible to refine F-Rosette to balance the stability and performance. For instance, the basic F-Rosette design only utilizes local links to for stable topology (Theorem 2). It is possible to extend F-Rosette with non-local links for lower latency (first proposed in [13]), by extending the base Rosette constellation in Figure 4b and construction in Algorithm 1

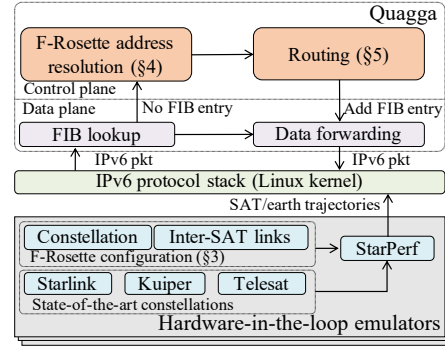


Figure 11: Hardware-in-the-loop experimental setup.

Table 3: F-Rosette under the same altitude and elevation angle of state-of-the-art mega-constellations.

	Number of satellites	Altitude H (km)	Inclination angle ϕ	Min. number of satellites in F-Rosette
Starlink	1584	550	53	676
Kuiper	1156	630	51.9	676
TeleSat	351	1015	98.98	225

with m -local links. In this case, the maximum number of hops in Theorem 6 can be reduced to $\frac{N(k+1)}{2m}$. The cost is more link failures (Theorem 2) and unstable routing. We are neutral to this tradeoff and leave it for the operators to decide.

7 EVALUATION

We evaluate the efficiency and overhead of F-Rosette’s network structure (§7.1), addressing (§7.2), and routing (§7.3).

Prototype: We prototype an IPv6-based F-Rosette satellite protocol suite with 13K lines of C code, as shown in Figure 11. We build F-Rosette on top of the standard IPv6 routing suite by extending Quagga 0.99.23 [40] and run it in a customized Linux 3.10.0 kernel (which resembles Starlink’s Linux-based small satellites [41]). At the control plane, we implement F-Rosette’s hierarchical addresses, and embed them into the IPv6 address as shown in Figure 7. We also implement F-Rosette’s routing algorithms in §5 to compute the FIB entry for a new incoming packet. At the data plane, we reuse the standard IPv6 routing table and forwarding engine for prefix-based F-Rosette routing in §5. At runtime, an IPv6 packet with F-Rosette address will be forwarded to the user plane. If the routing table does not have a FIB entry for this address, it will be relayed to the control plane. The control plane will parse the IPv6 address to get the F-Rosette address, run Algorithm 2–3 for this address, generate and install the FIB entry, and then forward the packet. Later packets with to the same destination will be directly forwarded by routing table lookup at the data plane.

Experimental setup: With our limited capability of launching massive satellites to space, we conduct a hardware-in-the-loop, trace-driven emulation to approximate the real space-ground networks. We use StarPerf [42] to approximate the mega-constellations based on F-Rosette’s setup in §3.2 and real TLE orbit information of Starlink [1], Kuiper [2], and Telesat [3] from Space-Track [43]. The emulator will generate

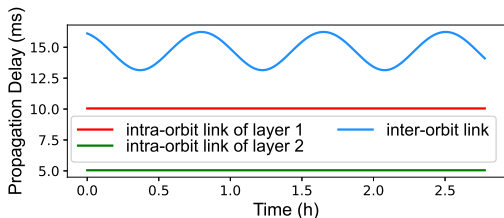


Figure 12: F-Rosette’s inter-satellite link delay in free space under J4 orbit propagation model [44, 45].

the runtime satellite motions, earth’s rotations, and inter-satellite link qualities (delay, loss, and capacity) based on the well-tested J4 orbit propagation model [44, 45] in aerospace engineering. For the projections in §2.2, we use a ThinkStation P910 workstation (22-core 3.5GHz Intel E5-2600, 64GB DDR4) with mininet [46] to create all virtual satellites in LEO mega-constellations. We also run our prototype on a testbed of 5 servers (with 2.2GHz CPU and 4GB memory usage limit to approximate the real small LEO satellites in [47, 48]) to quantify its data forwarding performance and overhead.

Ethics: This work does not raise any ethical issues.

7.1 Characteristics of F-Rosette Structure

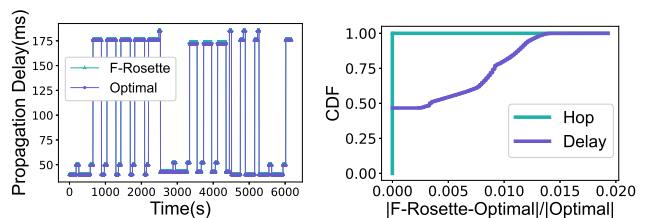
We first assess the F-Rosette’s network structure in §3.3, and compare them with existing mega-constellations.

Full coverage with fewer satellites: Table 3 compares F-Rosette with state-of-the-art mega-constellations under the same altitude and elevation angle. It confirms F-Rosette can achieve the same coverage as the state-of-the-art’s with 35.9–57.3% fewer satellites. This is mainly because F-Rosette is based on Rosette constellation, which typically requires less satellites than Walker-based constellations today [23]. Note existing mega-constellations may still achieve full coverage with fewer satellites. Besides, to satisfy F-Rosette’s construction, the actual number of satellites in F-Rosette can be slightly more than this minimum. This can be optimized by tuning the choices of N , m and k .

Stable network topology: F-Rosette’s stability under the minimum altitude H has been proven in Theorem 2. Table 2 quantifies H under different F-Rosette sizes. More satellites in F-Rosette generally lead to a lower altitude, thus facilitating low latency network services.

Geographical cells on the ground: Table 2 quantifies the number of geographical cells and their average sizes in F-Rosette with $N = 8$, $m = 6$. More geographical cells can be formed by increasing the number of layers k , thus offering fine-grained and faster network services.

Propagation delay of an inter-satellite link: Figure 12 exemplifies the RTT variance of links between two satellites with $N = 16$, $k = 1$ using J4 orbit perturbation [44, 45]. For intra-orbit links, F-Rosette ensures *fixed* one-hop RTT because of the fixed inter-satellite distance. For inter-orbit links, F-Rosette confirms periodic, predictive and bounded variance of the RTT, which is feasible for low-jitter applications.



(a) An example trace (b) Closeness to optimality

Figure 13: F-Rosette’s near-optimal routing.

Table 4: Header usage in F-Rosette’s address ($N = 16$).

	Num. satellites	Bits of row	Bits of column	Total bits
F-Rosette ₀	16	4	4	8
F-Rosette ₁	256	8	9	17
F-Rosette ₂	4096	12	14	26
F-Rosette ₃	65536	16	19	35

Compared to terrestrial networks, RTT between satellites is less noisy due to the laser communication in vacuum.

7.2 Network Addressing in F-Rosette

We next evaluate the network addressing in F-Rosette. It has been proved in §4 that F-Rosette does not incur satellite or user IP address changes in §2.2. Here we assess the efficiency and cost of F-Rosette address in IPv6.

Addressing efficiency: We quantify the packet space usage by F-Rosette’s address. Table 4 shows the header spaces needed inside an 128-bit IPv6 address to embed F-Rosette’s hierarchical address in §4. For satellites, a F-Rosette with $N = 16$ can support up to $k = 8$ (2^{32} satellites) with 32-bit address space. For ground cells, with a 32-bit address, a F-Rosette with $N = 16$ can support up to $k = 2$. More cells can be accommodated with more bits in 128-bit IPv6 address. Note users in the same geographical cell should be assigned different suffixes to avoid duplicate IPv6 address (§4.2). With 32-bit suffix in an IPv6 address, F-Rosette can support up to 2^{32} in each geographical cell, and leaves 64 bits as IPv6 prefixes for inter-networking to external networks.

Addressing overhead: At runtime, F-Rosette should process its address for Algorithm 2 (for satellites) or Algorithm 3 (for ground users). For the satellite address, F-Rosette performs the prefix/wildcard matching based on the standard FIB, thus retaining same cost as standard IPv6 with negligible overhead. For ground users, F-Rosette should map its geographical cell ID to the corresponding location (α, γ) . Table 6 confirms that the runtime table lookup time is marginal. Table 5 shows ≤ 2 MB is needed for the geographical ID-to-location table for $N = 16$, $k = 3$, which is acceptable even for small LEO satellites with limited storage.

7.3 Routing in F-Rosette

We last evaluate the routing in F-Rosette. It has been proven in §5 that F-Rosette does not incur routing re-convergence or suffer from low network usability in §2.2. So this section focuses on the routing efficiency and overhead.

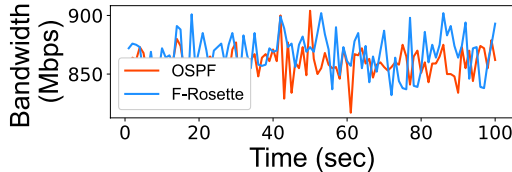


Figure 14: Data forwarding speed at 1Gbps links.

Table 5: Storage overhead with $N = 16$

	F-Rosette ₀	F-Rosette ₁	F-Rosette ₂	F-Rosette ₃
Memory (bytes)	64	1,984	61,504	1,906,624

Table 6: System overhead of F-Rosette.

CPU usage	< 1%
Memory usage	1344kB
1st packet’s processing latency	0.048–0.058ms
table lookup time	0.006–0.008ms
Bandwidth	867.42Mbps

Routing efficiency: We first compare F-Rosette’s routing in §5 with the paths with the shortest hop counts and propagation delays. In this experiment, we route traffic from Beijing to New York using F-Rosette with $N = 16, m = 2, k = 1$ (256 satellites) at the altitude of 878.76km. We compare F-Rosette’s hop counts and propagation delays with those in the shortest path. Figure 13 confirms that, F-Rosette always achieves the shortest path in hop counts as proved in Theorem 4. Due to the time-varying inter-orbit satellite link delays (Figure 12 and Equation 11), F-Rosette does not always find the shortest path in propagation delays. Even so, Figure 13b shows F-Rosette’s bounded link delay variances help F-Rosette approximates the optimal delay with $\leq 1.4\%$ difference, thus $\leq 1.62\text{ms}$. Note the spikes in Figure 13b arise from user’s handoffs between satellites, during which the user re-associates to a closer satellite. Despite this dynamics, F-Rosette still retains near-optimality compared to the shortest path in propagation delays.

Besides near-optimal routing path, F-Rosette’s forwarding engine also retains high data throughput. Figure 14 shows the end-to-end iperf throughput in a five-server testbed running F-Rosette over 1Gbps links. It confirms F-Rosette’s routing can saturate the physical bandwidth, and achieves comparable speed to the standard OSPF routing in IPv6. Since its routing algorithm can be realized with readily-available prefix/wildcard matching today, F-Rosette achieves comparable data forwarding performance to standard IP routing.

Routing overhead: Since F-Rosette runs atop IPv6, it incurs marginal cost compared to state-of-the-arts. Table 6 shows that the processing latency of the first packet with a new destination address is $\leq 0.058\text{ms}$ (for FIB setup). Later packets to the same destination will be directly forwarded by FIB lookup without this additional processing. Table 6 shows $< 1\%$ CPU and $\leq 1.3\text{MB}$ memory usage of F-Rosette under the same CPU/memory conditions as the LEO satellite’s, thus affordable for resource-constrained small satellites.

8 RELATED WORK

LEO satellite network has been actively studied for decades. Early efforts design constellations to ensure coverage, such as Walker [49], Rider [50], Rosette [23], Ellipso [51], to name a few. LEO satellites in these constellations are standalone, without forming a network in space. The first LEO network in operation is Iridium [9], a 66-satellite small constellation on the polar orbit. Since 2000s, various network designs have been proposed for Iridium, such as the location address [52–57], virtual node routing [21, 22], virtual topology routing [19, 20], multi-layer routing [58, 59], and geographical routing [30, 33, 60–62]. However, they cannot easily extend or scale to the mega-constellations as explained in §2.2. As mega-constellations are still at early adoptions, recent studies explore their performance optimization [63–65] or application to broader scenarios like navigation [66], in-orbit computing [48] and content delivery [38, 39]. [13] notices the link churns between satellites and proposes remedies, but it does not stabilize the network between space and ground. Instead, F-Rosette takes to first step to strive for a stable space-ground network in LEO mega-constellations.

F-Rosette is inspired by many network structure designs in other domains such as data center [67–69], P2P [70, 71], and wireless network [72–74]. It is based on the Rosette constellation [23], but generalizes it with a recursive structure and inter-satellite links. Its network addressing is inspired by classical geographical information systems like Google S2 [75] and Uber H3 [76], but customized for space-ground networking. F-Rosette’s geographical-to-topological routing embedding resembles greedy embedding [33, 34], but works in a different domain of space-ground network.

9 CONCLUSION

This work devises F-Rosette, a stable space-ground network structure in LEO mega-constellation. F-Rosette strives for stable network topology, address, and routing under dynamic many-to-many space-ground mapping in high mobility. F-Rosette’s recursive structure over the Rosette constellation guarantees provably stable network topology. Its hierarchical, geographical addressing embedded prevents the frequent address change for its users. F-Rosette does not incur global routing re-convergence in satellite mobility or earth’s rotations. To route traffic between users, F-Rosette performs efficient geographical routing by embedding it into the stable topological routing between satellites. F-Rosette is compatible with IPv6 and incrementally deployable.

F-Rosette is an initial effort to strive for a stable space-ground network at scale. Compared to the terrestrial network nodes, satellites are much harder to modify or upgrade once they are launched to space. Therefore, although the mega-constellations are still at early deployments, it is necessary

to systematically design the network before it is too late to change. We hope F-Rosette could call for the community's attention and stimulate more research efforts in this area.

REFERENCES

- [1] SpaceX Starlink. <https://www.starlink.com/>, 2021.
- [2] Amazon receives FCC approval for project Kuiper satellite constellation. <https://www.aboutamazon.com/news/company-news/amazon-receives-fcc-approval-for-project-kuiper-satellite-constellation>, 2020.
- [3] Telesat LEO satellites. <https://www.telesat.com/leo-satellites/>, 2021.
- [4] OneWeb constellation. <https://www.oneweb.world/>, 2021.
- [5] CNBC. SpaceX prices Starlink satellite internet service at \$99 per month, according to e-mail. <https://www.cnbc.com/2020/10/27/spacex-starlink-service-priced-at-99-a-month-public-beta-test-begins.html>, 2020.
- [6] Wccftech. SpaceX Successfully Tests Inter-Satellite Starlink Connectivity Via Lasers. <https://wccftech.com/spacex-starlink-satellite-laser-test/>, Sep 2020.
- [7] TheVerge. With latest Starlink launch, SpaceX touts 100 Mbps download speeds and "space lasers" (though the system still has a ways to go). <https://www.theverge.com/2020/9/3/21419841/spacex-starlink-internet-satellite-constellation-download-speeds-space-lasers>, 2020.
- [8] Inigo Del Portillo, Bruce G Cameron, and Edward F Crawley. A technical comparison of three low earth orbit satellite constellation systems to provide global broadband. *Acta Astronautica*, 159:123–135, 2019.
- [9] Zizhong Tan, Honglei Qin, Li Cong, and Chao Zhao. New method for positioning using iridium satellite signals of opportunity. *IEEE Access*, 7:83412–83423, 2019.
- [10] Wikipedia. Orbital Elements. https://en.wikipedia.org/wiki/Orbital_elements, 2021.
- [11] Elon Musk's twitter on IPv6 for Starlink.
- [12] Handley, Mark. Delay is Not an Option: Low Latency Routing in Space. In *Proceedings of the 17th ACM Workshop on Hot Topics in Networks (HotNet)*, pages 85–91. ACM, 2018.
- [13] Debopam Bhattacharjee and Ankit Singla. Network topology design at 27,000 km/hour. In *Proceedings of the 15th International Conference on Emerging Networking Experiments And Technologies*, pages 341–354, 2019.
- [14] NASA Socioeconomic Data and Applications Center (SEDAC). Gridded population of the world: Population count, v4.11 (2020). <https://sedac.ciesin.columbia.edu/data/set/gpw-v4-population-count-rev11>.
- [15] CNBC. Investing in space: SpaceX says Starlink internet has "extraordinary demand," with nearly 700,000 interested in service. <https://www.cnbc.com/2020/08/01/spacex-starlink-extraordinary-demand-with-nearly-700000-interested.html>, 2020.
- [16] Amazon AWS Ground station: Easily control satellites and ingest data with fully managed Ground Station as a Service. <https://aws.amazon.com/ground-station/>, 2021.
- [17] Microsoft Azure. New Azure Orbital, ground station as a service, now in preview. <https://azure.microsoft.com/en-us/updates/new-azure-orbital-ground-station-as-a-service-now-in-preview/>, 2020.
- [18] Pulak K Chowdhury, Mohammed Atiquzzaman, and William Ivancic. Handover schemes in satellite networks: state-of-the-art and future research directions. *IEEE Communications Surveys & Tutorials*, 8(4):2–14, 2006.
- [19] Markus Werner. A dynamic routing concept for atm-based satellite personal communication networks. *IEEE journal on selected areas in communications*, 15(8):1636–1648, 1997.
- [20] Hong Seong Chang, Byoung Wan Kim, Chang Gun Lee, Sang Lyu Min, Yanghee Choi, Hyun Suk Yang, Doug Nyun Kim, and Chong Sang Kim. Fsa-based link assignment and routing in low-earth orbit satellite networks. *IEEE transactions on vehicular technology*, 47(3):1037–1048, 1998.
- [21] Eylem Ekici, Ian F Akyildiz, and Michael D Bender. Datagram routing algorithm for leo satellite networks. In *Proceedings IEEE INFOCOM 2000. Conference on Computer Communications. Nineteenth Annual Joint Conference of the IEEE Computer and Communications Societies (Cat. No. 00CH37064)*, volume 2, pages 500–508. IEEE, 2000.
- [22] Eylem Ekici, Ian F Akyildiz, and Michael D Bender. A distributed routing algorithm for datagram traffic in leo satellite networks. *IEEE/ACM Transactions on networking*, 9(2):137–147, 2001.
- [23] Arthur H Ballard. Rosette constellations of earth satellites. *IEEE Transactions on Aerospace and Electronic Systems*, (5):656–673, 1980.
- [24] Lixia Zhang, Alexander Afanasyev, Jeffrey Burke, Van Jacobson, KC Claffy, Patrick Crowley, Christos Papadopoulos, Lan Wang, and Beichuan Zhang. Named data networking. *ACM SIGCOMM Computer Communication Review*, 44(3):66–73, 2014.
- [25] Van Jacobson, Diana K Smetters, James D Thornton, Michael F Plass, Nicholas H Briggs, and Rebecca L Braynard. Networking named content. In *Proceedings of the 5th international conference on Emerging networking experiments and technologies*, pages 1–12, 2009.
- [26] Xin Zhang, Hsu-Chun Hsiao, Geoffrey Hasker, Haowen Chan, Adrian Perrig, and David G Andersen. Scion: Scalability, control, and isolation on next-generation networks. In *2011 IEEE Symposium on Security and Privacy*, pages 212–227. IEEE, 2011.
- [27] Arun Venkataramani, James F Kurose, Dipankar Raychaudhuri, Kiran Nagaraja, Morley Mao, and Suman Banerjee. Mobilityfirst: a mobility-centric and trustworthy internet architecture. *ACM SIGCOMM Computer Communication Review*, 44(3):74–80, 2014.
- [28] Dongsu Han, Ashok Anand, Fahad Dogar, Boyan Li, Hyeontaek Lim, Michel Machado, Arvind Mukundan, Wenfei Wu, Aditya Akella, David G Andersen, et al. Xia: Efficient support for evolvable inter-networking. In *Presented as part of the 9th {USENIX} Symposium on Networked Systems Design and Implementation (NSDI 12)*, pages 309–322, 2012.
- [29] Stefan Ruehrup. Theory and practice of geographic routing. *Ad hoc and sensor wireless networks: architectures, algorithms and protocols*, 69, 2009.
- [30] Brad Karp and Hsiang-Tsung Kung. Gpsr: Greedy perimeter stateless routing for wireless networks. In *Proceedings of the 6th annual international conference on Mobile computing and networking*, pages 243–254. ACM, 2000.
- [31] Young-Jin Kim, Ramesh Govindan, Brad Karp, and Scott Shenker. Geographic routing made practical. In *Proceedings of the 2nd conference on Symposium on Networked Systems Design & Implementation-Volume 2*, pages 217–230. USENIX Association, 2005.
- [32] Ben Leong, Barbara Liskov, and Robert Tappan Morris. Geographic routing without planarization. In *NSDI*, volume 6, page 25, 2006.
- [33] Robert Kleinberg. Geographic routing using hyperbolic space. In *IEEE INFOCOM 2007-26th IEEE International Conference on Computer Communications*, pages 1902–1909. IEEE, 2007.
- [34] Simon S Lam and Chen Qian. Geographic routing in d -dimensional spaces with guaranteed delivery and low stretch. *IEEE/ACM Transactions on Networking*, 21(2):663–677, 2012.
- [35] AmericaSpace. 143-Strong Haul of Satellites Set for Sunday SpaceX Launch. <https://www.americaspace.com/2021/01/23/143-strong-haul-of-satellites-set-for-sunday-spacex-launch/>, 2021.
- [36] Vinton Cerf, Scott Burleigh, Adrian Hooke, Leigh Torgerson, Robert Durst, Keith Scott, Kevin Fall, and Howard Weiss. Delay-tolerant networking architecture. 2007.

- [37] Scott Burleigh, Adrian Hooke, Leigh Torgerson, Kevin Fall, Vint Cerf, Bob Durst, Keith Scott, and Howard Weiss. Delay-tolerant networking: an approach to interplanetary internet. *IEEE Communications Magazine*, 41(6):128–136, 2003.
- [38] Vaibhav Singh, Akarsh Prabhakara, Diana Zhang, Osman Yagan, and Swarn Kumar. A Community-Driven Approach to Democratize Access to Satellite Ground Stations. 2021.
- [39] Giacomo Giuliani, Tobias Klenze, Markus Legner, David Basin, Adrian Perrig, and Ankit Singla. Internet backbones in space. *SIGCOMM Comput. Commun. Rev.*, 50(1):25–37, 2020.
- [40] Quagga software routing suite. <https://www.quagga.net/>.
- [41] ZDNet. SpaceX: We’ve launched 32,000 Linux computers into space for Starlink internet. <https://www.zdnet.com/article/spacex-weve-launched-32000-linux-computers-into-space-for-starlink-internet/>, 2020.
- [42] Zeqi Lai, Hewu Li, and Jihao Li. Starperf: Characterizing network performance for emerging mega-constellations. In *2020 IEEE 28th International Conference on Network Protocols (ICNP)*, pages 1–11. IEEE, 2020.
- [43] Space Track. <https://www.space-track.org>, 2021.
- [44] Dirk Brouwer. Solution of the problem of artificial satellite theory without drag. Technical report, Yale University, 1959.
- [45] Yoshihide Kozai. The motion of a close earth satellite. *The Astronomical Journal*, 64:367, 1959.
- [46] Mininet.
- [47] Evan W Gretok, Evan T Kain, and Alan D George. Comparative benchmarking analysis of next-generation space processors. In *2019 IEEE Aerospace Conference*, pages 1–16. IEEE, 2019.
- [48] Debopam Bhattacharjee, Simon Kassing, Melissa Licciardello, and Ankit Singla. In-orbit computing: An outlandish thought experiment? In *Proceedings of the 19th ACM Workshop on Hot Topics in Networks*, pages 197–204, 2020.
- [49] J. G. Walker. Satellite Constellations. *Journal of the British Interplanetary Society*, 37:559, 1984.
- [50] L Rider. Analytic design of satellite constellations for zonal earth coverage using inclined circular orbits. *JAnSc*, 34:31–64, 1986.
- [51] David Castiel and John E Draim. The ellipso (tm) mobile satellite system. 1995.
- [52] A. Dainotti, K. Benson, A. King, B. Huffaker, E. Glatz, X. Dimitropoulos, P. Richter, A. Finamore, and A. C. Snoeren. Lost in space: Improving inference of ipv4 address space utilization. *IEEE Journal on Selected Areas in Communications*, 34(6):1862–1876, 2016.
- [53] Dan A Preston and Joseph Preston. Geo-spacial internet protocol addressing, May 22 2001. US Patent 6,236,652.
- [54] F Megen. Mapping universal geographical area description (gad) to ipv6 geo based unicast addresses. *Internet Draft*, 2001.
- [55] Tony Hain. An ipv6 provider-independent global unicast address format. *Internet Draft*, 2002.
- [56] A hybrid addressing method based on geographic location information. Patent.
- [57] A geographical zone ip addressing method of walker constellation network. Patent.
- [58] Chao Chen and Eylem Ekici. A routing protocol for hierarchical leo/meo satellite ip networks. *Wireless Networks*, 11(4):507–521, 2005.
- [59] Jae-Wook Lee, Jun-Woo Lee, Tae-Wan Kim, and Dae-Ung Kim. Satellite over satellite (sos) network: a novel concept of hierarchical architecture and routing in satellite network. In *Proceedings 25th Annual IEEE Conference on Local Computer Networks. LCN 2000*, pages 392–399. IEEE, 2000.
- [60] Thomas R Henderson and Randy H Katz. On distributed, geographic-based packet routing for leo satellite networks. In *Globecom’00-IEEE. Global Telecommunications Conference. Conference Record (Cat. No. 00CH37137)*, volume 2, pages 1119–1123. IEEE, 2000.
- [61] Simon S Lam and Chen Qian. Geographic routing in d-dimensional spaces with guaranteed delivery and low stretch. *ACM SIGMETRICS Performance Evaluation Review*, 39(1):217–228, 2011.
- [62] Ananth Rao, Sylvia Ratnasamy, Christos Papadimitriou, Scott Shenker, and Ion Stoica. Geographic routing without location information. In *Proceedings of the 9th annual international conference on Mobile computing and networking*, pages 96–108. ACM, 2003.
- [63] Tobias Klenze, Giacomo Giuliani, Christos Pappas, Adrian Perrig, and David Basin. Networking in heaven as on earth. In *Proceedings of the 17th ACM Workshop on Hot Topics in Networks*, pages 22–28, 2018.
- [64] Debopam Bhattacharjee, Waqar Aqeel, Ilker Nadi Bozkurt, Anthony Aguirre, Balakrishnan Chandrasekaran, P Brighten Godfrey, Gregory Laughlin, Bruce Maggs, and Ankit Singla. Gearing up for the 21st century space race. In *Proceedings of the 17th ACM Workshop on Hot Topics in Networks*, pages 113–119, 2018.
- [65] Mark Handley. Using ground relays for low-latency wide-area routing in megaconstellations. In *Proceedings of the 18th ACM Workshop on Hot Topics in Networks*, pages 125–132, 2019.
- [66] Sujay Narayana, R Venkatesha Prasad, Vijay Rao, Luca Mottola, and T Venkata Prabhakar. Hummingbird: energy efficient gps receiver for small satellites. In *Proceedings of the 26th Annual International Conference on Mobile Computing and Networking*, pages 1–13, 2020.
- [67] Chuanxiong Guo, Guohan Lu, Dan Li, Haitao Wu, Xuan Zhang, Yunfeng Shi, Chen Tian, Yongguang Zhang, and Songwu Lu. Bcube: a high performance, server-centric network architecture for modular data centers. In *Proceedings of the ACM SIGCOMM 2009 conference on Data communication*, pages 63–74, 2009.
- [68] Chuanxiong Guo, Haitao Wu, Kun Tan, Lei Shi, Yongguang Zhang, and Songwu Lu. Dcell: a scalable and fault-tolerant network structure for data centers. In *Proceedings of the ACM SIGCOMM 2008 conference on Data communication*, pages 75–86, 2008.
- [69] Albert Greenberg, James R Hamilton, Navendu Jain, Srikanth Kandula, Changhoon Kim, Parantap Lahiri, David A Maltz, Parveen Patel, and Sudipta Sengupta. VL2: A scalable and flexible data center network. In *Proceedings of the ACM SIGCOMM 2009 conference on Data communication*, pages 51–62, 2009.
- [70] Ion Stoica, Robert Morris, David Karger, M Frans Kaashoek, and Hari Balakrishnan. Chord: A Scalable Peer-to-Peer Lookup Service for Internet Applications. *ACM SIGCOMM Computer Communication Review*, 31(4):149–160, 2001.
- [71] Sylvia Ratnasamy, Paul Francis, Mark Handley, Richard Karp, and Scott Shenker. A scalable content-addressable network. In *Proceedings of the 2001 conference on Applications, technologies, architectures, and protocols for computer communications*, pages 161–172, 2001.
- [72] Matthias Grossglauser and David NC Tse. Mobility increases the capacity of ad hoc wireless networks. *IEEE/ACM transactions on networking*, 10(4):477–486, 2002.
- [73] Suhas N Diggavi, Matthias Grossglauser, and David N C Tse. Even one-dimensional mobility increases ad hoc wireless capacity. In *Proceedings IEEE International Symposium on Information Theory*, page 352. IEEE, 2002.
- [74] Xia Zhou, Zengbin Zhang, Yibo Zhu, Yubo Li, Saipriya Kumar, Amin Vahdat, Ben Y Zhao, and Haitao Zheng. Mirror mirror on the ceiling: Flexible wireless links for data centers. *ACM SIGCOMM Computer Communication Review*, 42(4):443–454, 2012.
- [75] Google S2 geometry library. <https://s2geometry.io/>, 2021.
- [76] H3: Uber’s Hexagonal Hierarchical Spatial Index. <https://s2geometry.io/>, 2021.

Algorithm 4 On-demand F-Rosette size selection.

Input: Ground-to-satellite round-trip demand RTT, minimum elevation angle ϕ
Output: The minimum number of layers k and satellites N_k for F-Rosette to guarantee full coverage

- 1: Compute satellite altitude $H = c \cdot \text{RTT}/2$;
- 2: Find each satellite's minimum coverage R_{min} in the unit of great circle range:

$$\tan \phi = \frac{\cos R_{min} - R_E/(R_E + H)}{\sin R_{min}}$$

- 3: Decide the minimum number of satellites to guarantee full coverage:

$$\sec R_{min} = \sqrt{3} \tan \left(\frac{\pi}{6} \frac{N_{min}}{N_{min} - 2} \right)$$

- 4: Decide the minimum number of layers k for F-Rosette:

$$k = \lceil \log_N N_{min} \rceil - 1$$

- 5: Decide the minimum number of satellites in F-Rosette: $N_k = N^{k+1}$;
-

A PROOF OF THEOREM 1

PROOF. By construction, F-Rosette guarantees the full coverage by following the condition for Rosette constellation [23]. With N^{k+1} satellites in a F-Rosette $_k$, Equation 6 in §3.1 has shown it suffices for each satellite with coverage $R = \sec^{-1} \left(\sqrt{3} \tan \left(\frac{\pi}{6} \frac{N^{k+1}}{N^{k+1} - 2} \right) \right)$ to guarantee full coverage. Given this per-satellite coverage R and elevation angle ϕ , the minimum altitude that a satellite can achieve this satellite is given by Equation 5. Therefore, we have $H_{min} = R_E \left(\frac{1}{\cos R - \sin R \tan \phi} - 1 \right)$. \square

B ON-DEMAND F-ROSETTE SIZE SELECTION

A satellite operator can choose the proper F-Rosette size that can ensure full coverage *and* meet its network latency demands. Algorithm 4 illustrates the size selection based on the ground-to-space round trip latency demand RTT, and the minimum elevation angle ϕ (constrained by the satellite and device hardware's capability). The operator can first specify the desired altitude of the satellites $H = c \cdot \text{RTT}/2$, where c is the light speed through the atmosphere. With the minimum elevation angle ϕ , one we derive the minimal per-satellite coverage R_{min} in the unit of great circle range: $\tan \phi = \frac{\cos R_{min} - R_E/(R_E + H)}{\sin R_{min}}$. With R_{min} the operator can derive the minimal number of satellites needed for a Rosette constellation to guarantee full coverage: $\sec R_{min} = \sqrt{3} \tan \left(\frac{\pi}{6} \frac{N_{min}}{N_{min} - 2} \right)$. Then given the F-Rosette $_0$ parameter N , the operator can choose the level of F-Rosette as $k = \lceil \log_N N_{min} \rceil - 1$.

C PROOF OF THEOREM 2

PROOF. To ensure the inter-satellite links are always on, the altitudes of the satellites should be sufficiently high for mutual visibility. To derive the minimum altitude, we first

compute the great circle range r_{ij} of satellite i and j from Equation 12. When r_{ij} is maximized, the distance between the two satellites reaches the maximum, which requires the highest altitude for mutual visibility. Therefore, if we want to prevent the link from passing through the earth, the condition that needs to be met is $(H + R_E) > \frac{R_E}{\cos \frac{r_{max}}{2}}$, where

$$\begin{aligned} \sin^2(r_{max}) &= \cos^4(\beta/2) \sin^2 m(m+1)(\pi/N) \\ &\quad + 2 \sin^2(\beta/2) \cos^2(\beta/2) \sin^2 m^2(\pi/N) \\ &\quad + \sin^4(\beta/2) \sin^2 m(m-1)(\pi/N) \\ &\quad + 2 \sin^2(\beta/2) \cos^2(\beta/2) \sin^2 m(\pi/N) \end{aligned}$$

Moreover, to guarantee full coverage, we require $H > H_{min}$. This ends up with $H > \max \left\{ \left(\frac{1}{\cos \frac{r_{max}}{2}} - 1 \right) R_E, H_{min} \right\}$. \square

D PROOF OF THEOREM 3

PROOF. We first note that each F-Rosette cell is a unique quadrilateral bounded by four satellite sub-point trajectories (two pairs of parallel spherical edges). To prove Theorem 3, it is sufficient to prove that when constructing F-Rosette $_k$ out of F-Rosette $_{k-1}$, each F-Rosette $_{k-1}$ cell will be intersected by $N - 2$ new satellite sub-point trajectories parallel to two of its edges, and another $N - 2$ satellite sub-point trajectories parallel to the other two of its edges. In this way, this F-Rosette $_{k-1}$ cell is divided into N^2 cells in F-Rosette $_k$. To prove this, consider a F-Rosette $_{k-1}$ cell bounded by the satellite sub-point trajectories of satellite S_i, S_{i+1}, S_j and S_{j+1} , as shown in Figure 6b. Recall the satellite sub-point trajectory for a satellite S_i in F-Rosette $_{k-1}$ in Equation 8–9. To construct F-Rosette $_{k-1}$ out of F-Rosette $_k$, each satellite S_i in F-Rosette $_{k-1}$ is replicated N times, each being shifted by a uniform time interval $t_k = \frac{T_s}{N^k}, k = 0, 1, 2, \dots, N - 1$. Note $t_0 = 0$ overlaps with S_i 's satellite sub-point trajectory. For each of the remaining replicated satellite S_i^k , its satellite sub-point trajectory is thus shifted by t_k (dotted lines in Figure 6b), which is between the satellite sub-point trajectories of S_i and S_{i+1} . Similar divisions apply to satellite S_j and S_{j+1} . So we conclude that this F-Rosette $_{k-1}$ cell is divided into N^2 F-Rosette $_k$ cells. However, some F-Rosette $_k$ cells near the polar regions do not belong to any F-Rosette $_{k-1}$ cells, so we artificially add two latitude lines equal to the inclination angle to form some F-Rosette $_{k-1}$ cells. These cells will be divided into $\frac{N^2 + N}{2}$ F-Rosette $_k$ cells. In order to satisfy this theorem, we will calculate some small cells repeatedly in the big cell. \square

E PROOF OF THEOREM 5

PROOF. Consider a satellite $S = s_0, s_1, \dots, s_k$ in a F-Rosette $_k$. At each layer $j \in [0, k - 1]$, S belongs to a ring topology of N

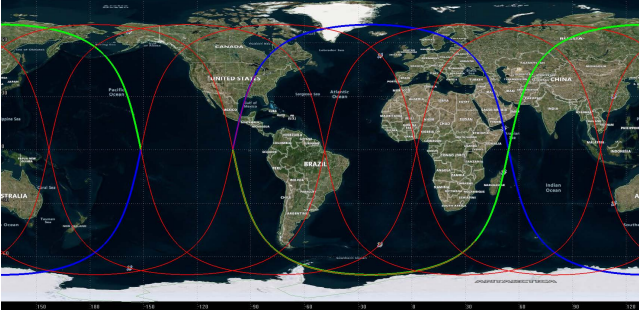


Figure 15: cells number in F-Rosette.

satellites according to F-Rosette's construction. According to Algorithm 2, these N satellites are divided into 2 groups based on S 's shortest path to them: one group is routed via clockwise routing, and the other group is routed via counter-clockwise routing. All satellites in the same group share the same next hop at S , so they can be aggregated in the FIB. Therefore, the number of FIB entries S needs at layer j is the number of prefixes that $(s_j, s_j + \frac{N}{2} \bmod N)$ and $(s_j + \frac{N}{2} \bmod N, s_j]$ can be aggregated into, which are both $\lceil \log \frac{N}{2} \rceil$. So S needs $2 \lceil \log \frac{N}{2} \rceil$ FIB entries for layer j . Since there are $k + 1$ layers in a F-Rosette $_k$, each satellite needs $2(k + 1) \lceil \log \frac{N}{2} \rceil$ FIB entries. \square

F PROOF OF LEMMA 1

PROOF. We show that a F-Rosette $_0$ has $(N - m)^2$ cells. Then according to Theorem 3, a F-Rosette $_k$ has $(N - m)^2 N^{2k}$ cells. First note F-Rosette's repeat ground-track orbits dedicate $T_E = (N - m)T$, i.e., after an orbital period T , the earth rotates $\frac{1}{N - m}$ of the great circle. So it takes $(N - m)T$ for a satellite in F-Rosette $_0$ to revisit the place it passed before. Based on the repetitions of the orbit period, a satellite's sub-point trajectory can be divided into $N - m$ parts $\{C_i, i = 1, 2, \dots, N - m\}$. As Figure 15 exemplifies, the blue curve is one of C_i , and curves will intersect to form cells. We can uniquely identify a cell with its left vertex since the number of the vertexes is equal to the number of the cells (Euler theorem). Because of the earth's rotation, there are 1 curve that do not intersect with C_i (green curve in Figure 15). Besides, C_i has $2(N - m - 2)$ intersections with others (excluding itself). So there are $(N - m)(N - m - 2)$ intersections in total. In addition, with the maximum latitudes a F-Rosette $_0$ can cover (constrained by the satellites' inclination angle β), two more rows exist at these latitudes and add the total number of cells to $(N - m)^2$. So according to Theorem 3, a F-Rosette $_k$ has $(N - m)^2 N^{2k}$ cells. \square

G PROOF OF THEOREM 7

PROOF. We prove this theorem by recursion. When $k = 0$, there are always $2(k + 1) = 2$ disjoint paths between any

two satellites (one clockwise, the other counter-clockwise as exemplified in Figure 4b). Assume there are $2(k + 1)$ disjoint paths for a F-Rosette $_k$. Now consider a F-Rosette $_{k+1}$ and two satellites $S = s_0.s_1 \dots s_k.s_{k+1}$ and $D = d_0.d_1 \dots d_k.d_{k+1}$. The following $k + 2$ routes enumerate all disjoint paths from S to D :

$$s_0.s_1 \dots s_k.s_{k+1} \rightarrow d_0.s_1 \dots s_k.s_{k+1} \rightarrow d_0.d_1 \dots d_k.d_{k+1}$$

$$s_0.s_1 \dots s_k.s_{k+1} \rightarrow s_0.d_1 \dots s_k.s_{k+1} \rightarrow d_0.d_1 \dots d_k.d_{k+1}$$

...

$$s_0.s_1 \dots s_k.s_{k+1} \rightarrow s_0.s_1 \dots s_k.d_{k+1} \rightarrow d_0.d_1 \dots d_k.d_{k+1}$$

For each route, the first hop has 2 disjoint paths (one clockwise, the other counter-clockwise), and the second hop has $2(k + 1)$ disjoint paths. So each route forms $\min(2, 2(k + 1)) = 2$ disjoint paths. Since each two routes above do not overlap, we end up with $2(k + 2)$ disjoint routes from S to D and thus conclude this proof by recursion. \square

H GEOGRAPHICAL CELL ID-TO-LOCATION TABLE

A key prerequisite in Algorithm 3 is to decide the destination cell's geographical location (α, γ) given its ID $c_0.c_1 \dots c_k$ for each packet. This section describes how to accelerate this operation via table lookup.

Table structure: Figure 9 illustrates the mapping table from geographical cell ID $c_0.c_1 \dots c_k$ to its location (α, γ) (defined as its left vertex). As we will see, this table only needs to store α and γ can be derived from α . A F-Rosette $_k$ constructs one table for level 0, and $\frac{(N - m)N^{i-1}}{2}$ tables for level $i = 1, 2, \dots, k$. Each table contains two columns, indicating the row index $c_j.row_j$ and the corresponding coordinate of the first cell in each row α_0 . The row of the previous level plus its index multiplied by N represents the index of the next level table. For any other cell i in this row, its coordinate can be derived as $\alpha_j = \alpha_0 + \frac{2\pi j}{(N - m) \cdot N^k}$ according to F-Rosette's construction. Each cell i 's phase shift $\gamma_j \equiv (N - m)\alpha_0$.

Table pre-computation: To pre-compute the mapping table, the key step is to learn α_0 for each row. To derive α_0 , we have two observations. First, all cells in F-Rosette are formed by the satellite sub-point trajectories, so α_0 can be derived from Equation 8-9. Second, F-Rosette guarantees all satellites traverse the same stable sub-point trajectories and thus cells (§3.1-3.2). So α_0 can be learned by tracking any satellite in F-Rosette. For simplicity, we derive α_0 from the first satellite (0.0...0) in F-Rosette as $\alpha_0 = \omega_E t$. According to Equation 9, its sub-point trajectory is:

$$\tan(\lambda + \omega_E t) = \cos \beta \cdot \tan(m\omega_E t)$$

From t to $t + T$, this satellite passes through all rows of cells with an increment of longitude $\Delta\lambda/2$, where $\Delta\lambda = \frac{2\pi}{(N - m) \cdot N^k}$

Algorithm 5 Mapping geographical cell ID to its location in F-Rosette.

Input: Cell ID $c_0.c_1\dots.c_k$. N , m , k , table lists of α_0 $Table_i, i = 0, 1, \dots, k$, each $Table_i$ is a list of tables, target level of cell k_0

Output: Geographical location (α, γ)

```

1: index = 0; ▷ Index in table list, indicates which table to look up
2:  $\Delta\alpha = c_0.col \cdot \frac{2\pi}{N(N-m)}$ ;
3: for i=1 to  $k_0$  do
4:   index = index · N +  $c_{i-1}.row$ ;
5:    $\Delta\alpha = \Delta\alpha + c_i.col \cdot \frac{2\pi}{(N-m)Ni}$ ;
6: end for
7:  $T = Table_{k_0}[index]$ ; ▷ The table to look up
8:  $\alpha_0 = T[c_{k_0}.row]$ ; ▷ Get the  $\alpha_0$  from table T
9:  $\alpha = \alpha_0 + \Delta\alpha; \gamma = (N - m)\alpha_0$ ;
10: return  $(\alpha, \gamma)$ ;

```

is the longitude difference between adjacent cells. So given $\Delta\lambda/2$ and T , we numerically search all the time t that satisfies the above equation, and then get $\alpha_0 = \omega_E t$.

Hierarchical table lookup: To learn the location (α, γ) from a geographical cell ID $c_0.c_1\dots.c_k$, a satellite hierarchically searches the mapping table level-by-level. Algorithm 5 illustrates the table lookup procedure. F-Rosette maintains the accumulative relative position $\Delta\alpha$ to the first cell in each row α_0 . Starting from the first level, F-Rosette iteratively updates $\Delta\alpha$ and decides the table it should search in the next level. Then this cell's location is decided as $\alpha = \alpha_0 + \Delta\alpha, \gamma = (N - m)\alpha_0$.

Storage and lookup cost: Both are modest for the small LEO satellites. With one entry per geographical row, a satellite should store $\frac{(N-m)N^k}{2}$ entries in the table (e.g., $\approx 2\text{MB}$ as shown in Table 5). The table lookup traverses one row per F-Rosette level, resulting in a $O(k + 1)$ lookup complexity.